Three Dimensional Calculation of Magnetic Forces and Displacements of a Claw-Pole Generator

I. Ramesohl, G. Henneberger, S. Küppers and W. Hadrys
Institute of Electrical Machines, University of Technology Aachen, Schinkelstrasse 4, 52056 Aachen, Germany

***Abstract*—This paper deals with the procedure of calculating the vibration of a claw-pole generator. The stimulating forces of magnetic origin are calculated for several speeds. For the calculation of the displacements the total generator system (stator plates with windings and housing) is taken into account. The displacement magnitude of the housing surface mainly causes the audible noise. The procedure makes it possible to ascertain the vibratory condition of an electrical machine just by means of the design and material data. Some results of stator vibration are presented and compared with measurements.**

I. Introduction

The claw-pole alternator supplies the energy for many electric consumers of an automobile. Going along with noise reduction of combustion engines, the audible noise of the generator becomes more and more important. The time behaviour of the magnetic force density can be computed with the knowledge of the magnetic field vectors in the time domain. These time intervals are first transformed into a mechanical model (360^0) and then transformed to the frequency domain. The spectral components of the force are input quantities for the dynamic displacement calculation. The procedure is done for two different claw-pole alternator types. Fig. 1 shows one pole pitch of model 1 at which the vibrations can be measured at the stator while the machine is in operation. The comparison of computation and measurements is presented for one alternative of material condition. The geometry of the magnetic part of model 2, a machine out of series production, is shown in Fig. 2. Some results of the evolution of the transient response of the magnetic forces under load with variable speed will be demonstrated at this model.

Later the displacement data can also be used to compute the noise level at discret points.

Manuscript received July 10, 1995.

I. Ramesohl, e-mail: ramesohl@iem.rwth-aachen.de;
G. Henneberger, e-mail: henneberger@rwth-aachen.de

II. Calculation of magnetally forced vivration

The calculation of the magnetally forced vibration is divided into three parts: At first the transient behaviour of the magnetic field vectors is calculated. Subsequently the force density at the stator surface is determined and transformed into the spectral mode. At last the components of force are used as forward signals for the displacement calculation.

A. Magnetic field calculation

Typically the generator has 12 poles and 36 teeth with a three-phase winding in the stator. To analyse the field in

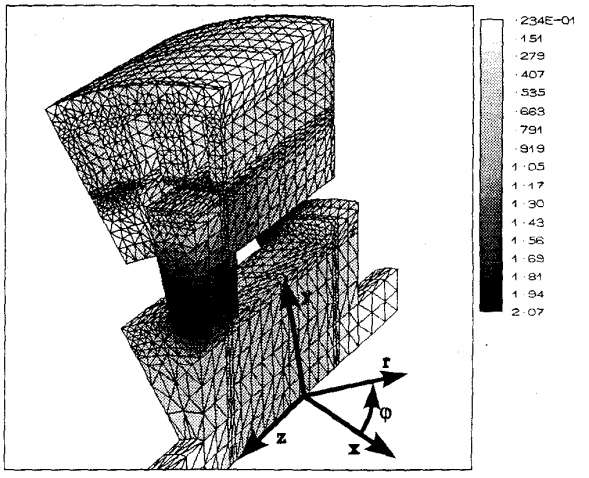

Fig. 1. Magnetic flux density distribution (model 1) in Tesla

one pole-pitch, a magnetic field computation at 5 stator-rotor positions is carried out. The FE-mesh contains about 13,000 nodes and 70,000 tetrahedras. Using the periodic condition there is a total of 30 time steps for one period of the flux density at every node in the stator which allows a calculation up to the 14th harmonic in the frequency domain.

The 3d magnetostatic field calculation is done using the commercial FE-program MagNet3D [2], [3]. The CPU-time on a hp9000/735 workstation for one problem under load is about 3 h with three to four iteration steps for

the rotor displacement angle and the stator current. The equation concerning the periodical condition of the scalar potential takes the following form:

$$V_m(r, \varphi + \Delta\varphi, -z) = -V_m(r, \varphi, z), \quad (1)$$

where $\Delta\varphi = 30^0$ is the angle of one pole-pitch (see Fig. 1 for the position of the system coordinates). The conditions of the magnetic flux density are given in (2,3):

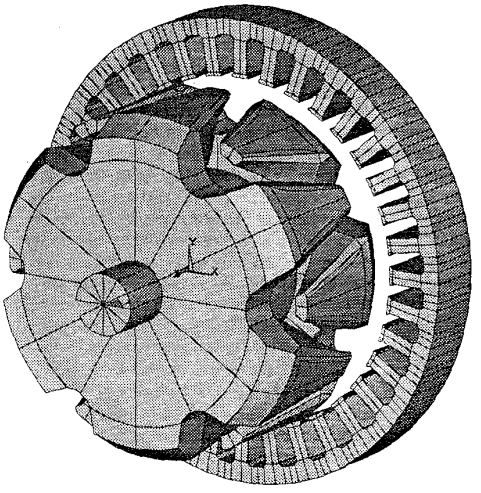

Fig. 2. Surface plot of the full magnetic part of model 2

$$B_{r,\varphi}(r, \varphi + \Delta\varphi, -z) = -B_{r,\varphi}(r, \varphi, z) \quad (2)$$

$$B_z(r, \varphi + \Delta\varphi, -z) = B_z(r, \varphi, z). \quad (3)$$

The results of the magnetic flux at no-load of one stator-rotor position of model 1 is shown in Fig 1. This machine has an unfavourable geometric shape because of high saturation in the claw-pole rotor up to 2 Tesla. Model 2 shows a better magnetic capacity and a higher output current in comparison to model 1.

B. Force density calculation

An expression for the local surface force density is given by the Maxwell's stress tensor:

$$\vec{\sigma} = \frac{1}{2}\vec{n}_{12}[B_n(H_{1n} - H_{2n}) - (w_1' - w_2')], \quad (4)$$

where n stands for the normal components of the field vectors $\vec{B}$ and $\vec{H}$ [1]. The vector $\vec{n}_{12}$ represents the normal of the boundary surface from region 2 to 1 and w_1' w_2' are the magnetic co-energie densities [1]. At the no-load case it is not necessary to take the Lorenz forces into consideration because the stator conductors are without current. At load they are much smaller than the boundary force at the stator teeth. Furthermore the influence of magnetistriction is not taken into account.

In comparison with (4,5) the periodical conditions of the force densities change their sign in the following form (because they are periodic in one pole-pitch):

$$\sigma_{r,\varphi,z}(r, \varphi + \Delta\varphi, -z) = \sigma_{r,\varphi,z}(r, \varphi, z). \quad (5)$$

Fig. 3 shows the absolute values of force-density calculation at the stator surface of model 2 under load by 6000 rpm . The maximum values are in the near of the edges while the claws move from right to left.

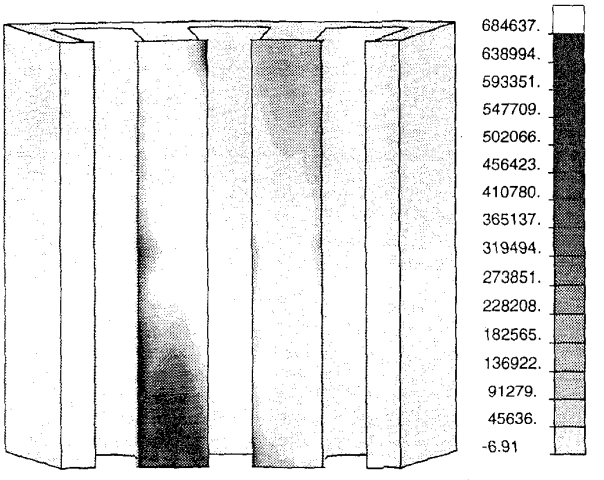

Fig. 3. Distribution of the magnetic force densities at the stator surface under load at 6000 rpm in N/m^2

The evolution of the global forces of model 2 in radial direction is shown in Fig 4. The forces belong to one tooth-pitch as function of thirty discret time steps and they are an numerical intergration of all nodes in this region. Also the influence of the generator speed can be seen. The maximum values of F are at lower speeds of about 1500 - 2400 rpm because of less armature reaction in this speed range. The evolution of the spectral

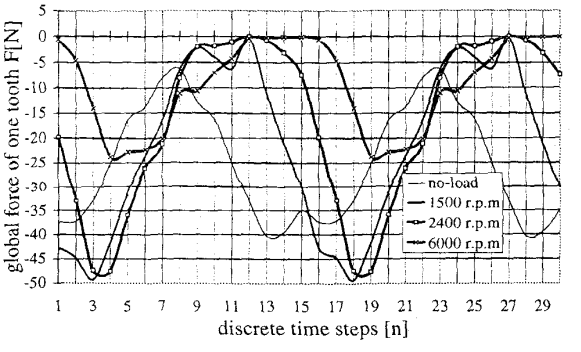

Fig. 4. Evolution of the global forces of model 2 in radial direction

components of these integral forces of one tooth-pitch is shown in Fig 5 for some more speeds. An extract of the

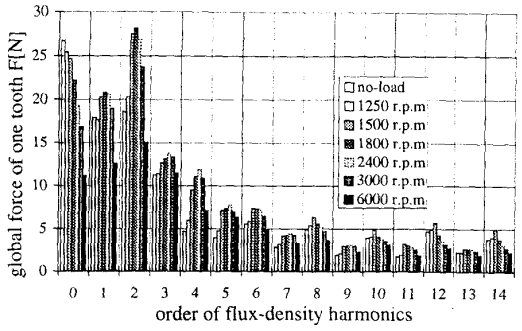

Fig. 5. Evolution of the harmonics of the global forces of model 2 in radial direction

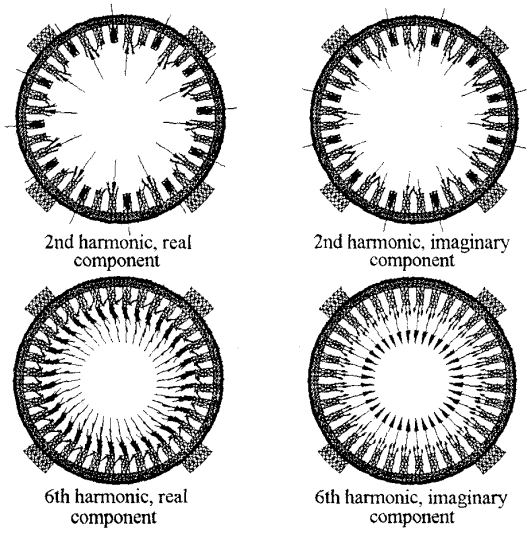

Fig. 6. Distribution of the magnetic forces at the stator of model 1

global results of model 1 is shown in Fig. 6 where the spectral components have already been transformed to a three dimensional mechanical model of the stator. There are presented several node levels in axial direction in this picture. The special geometry of the stator with rectangular claws ($\alpha_i = 2/3$) and stator teeth (60^0) leads to the neglecting of all odd spectral components here in contrast to model 2.

C. Calculation and measurement of deformation

The general equation of motion of a discretized structure in finite element formulation can be expressed in the following form [1]:

$$(\underline{K} + j \cdot \omega \cdot \underline{F} - \omega^2 \cdot \underline{M}) \cdot \hat{D} = \alpha \cdot \hat{\underline{R}} \qquad (6)$$

where $\underline{D}$ is the generalized displacement vector, $\underline{M}$ the generalized mass matrix, ω the mechanical angular velocity, $\hat{\underline{R}}$ the generalized force vector, α is an anisotropie coefficient and $\underline{F}$ is the damping matrix which is neglected here. This neglecting is only admissible if ω is far from the resonance pulsation of the structure.

Fig. 7 shows the results of a separate calculation of the displacements of the stator at a speed of 3000 rpm. In this computation of vibration the suspension clips of

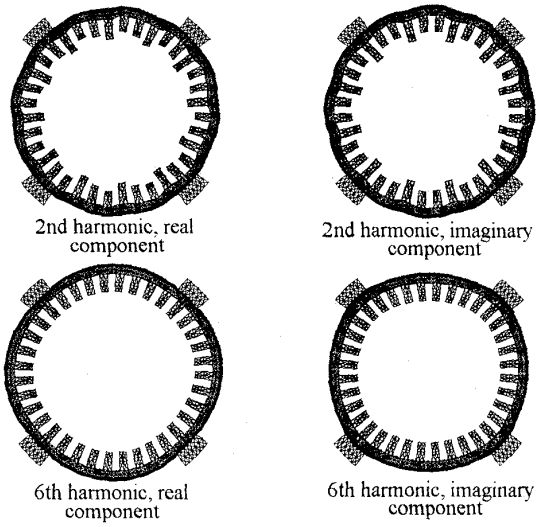

Fig. 7. Displacement results of a separate calculation of the stator

the stator are prevented from movement. In this case all corresponding lines and columns of the generalized displacement vector in (6) are set to zero.

The stator is of laminated structure. Many authors have shown already that these laminated components are more flexible than their solid counterparts and that this fact has a strong bearing on the level of vibration. Therefore it seems necessary to introduce a transversely-isotropic material for the stator. Then the generalized Hook's law, for a coordinate system, in which the z-axis is in axial direction of the machine, can be written [4]:

$$\begin{pmatrix} \sigma_x \\ \sigma_y \\ \sigma_z \\ \tau_{xy} \\ \tau_{yz} \\ \tau_{zx} \end{pmatrix} = \underline{H} \cdot \begin{pmatrix} \varepsilon_x \\ \varepsilon_y \\ \varepsilon_z \\ \gamma_{xy} \\ \gamma_{yz} \\ \gamma_{zx} \end{pmatrix} \qquad (7)$$

$$\underline{H} = \begin{pmatrix} h_{11} & h_{21} & h_{31} & 0 & 0 & 0 \\ h_{21} & h_{11} & h_{31} & 0 & 0 & 0 \\ h_{31} & h_{31} & h_{33} & 0 & 0 & 0 \\ 0 & 0 & 0 & \frac{1}{2}(h_{11} - h_{21}) & 0 & 0 \\ 0 & 0 & 0 & 0 & h_{55} & 0 \\ 0 & 0 & 0 & 0 & 0 & h_{55} \end{pmatrix} \qquad (8)$$

$\underline{H}$ is used to calculate the generalized stiffness matrix $\underline{K}$ in equation 6 [1]. Fig. 8 shows the test bench in order to measure the vibration behaviour with fixed clambing of

the suspension clips of the stator. The bearing of the rotor is separated from the stator in order to get a vibration isolation. It is measured with an accelerator which has a mass of 5g and a width which is equivalent to about one tooth-pitch. The spectrum of vibration has been measured and can be compared to calculations. The deformation contour of the 6th harmonic in radial direction at the stator surface at 3000 rpm, which causes the most acoustic problems, is compared to the computation in Fig 9. Furthermore the unrolled stator is shown in this picture. The material parameters, which are used for the calculation in Fig 9 are only admissible for the radial direction. They are presented in Table I. More accurate material properties could be found out by experimental material testing. The measurement of vibration in axial direction is difficult because of small supporting surface of the stator.

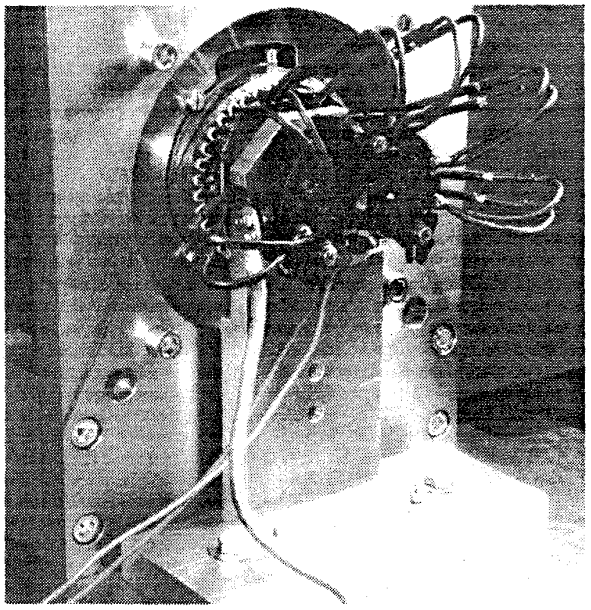

Fig. 8. Test bench with stator windings and diode plate

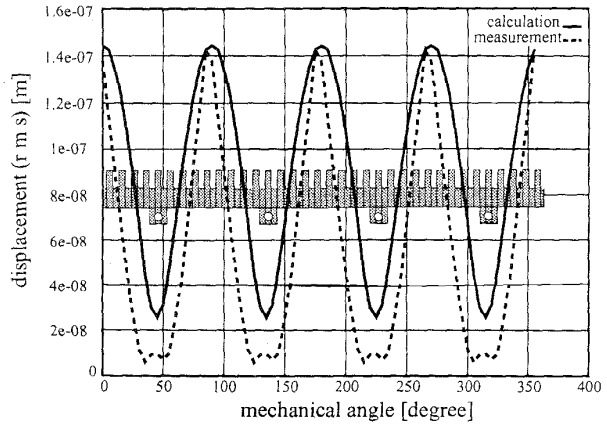

Fig. 9. Displacement of the 6th harmonic in radial direction

TABLE I

Material properties of the stator used in Fig 9

h_{11}	=	$8.30 \cdot 10^9 N/m^2$
h_{21}	=	$2.48 \cdot 10^9 N/m^2$
h_{31}	=	$2.48 \cdot 10^9 N/m^2$
h_{33}	=	$8.30 \cdot 10^9 N/m^2$
h_{55}	=	$2.91 \cdot 10^9 N/m^2$
ρ	=	$7.50 \cdot 10^3 kg/m^3$

III. Conclusion

A procedure to calculate the magnetic forced vibration of the claw-pole generator is described in this paper. It is possible to calculate the time behaviour of the surface force density for any speeds and excitations depending on the magnetic field computation. The time functions of the forces can be transformed to a mechanical model of the generator and are used as input quantities for the dynamic calculation of deformation. It is difficult to find out the material properties of the laminated structure of the stator. This makes it necessary to concentrate on the vibrational behaviour of the stator at first. A suitable test bench is created in order to lead a parameter identification for the laminated stator package. Static measurements are planned for the future.

The results of the computations are compared to measurements of vibration but the small supporting surface of the package does not allow to scan all points with an accelerator. The most audible noise of magnetally origin of a claw-pole generator is caused by the 5th and 6th harmonic. This procedure of calculation with the FE-method and the described measurement are an usefull practice to investigate these components.

References

[1] W. Hadrys, "Elektromagnetische, mechanische und akustische Berechnung von Induktionstiegelöfen zur Geräuschreduzierung", *Shaker*, Dissertation, RWTH Aachen, 1995.

[2] Webb J.P., Forghani B., "A single scalar potential method for 3D Magnetostic using edge elements", *IEEE Trans. Magn.*, Vol. 25, pp. 4126-4128, September 1989.

[3] G. Henneberger,S. Küppers, R. Block, "Feldberechnung und Simulation eines Klauenpolgenerators", *Arch. Elektrotechnik*, No 76, 1993.

[4] S.G. Lekhnitskii, "Anisotropic Plates", *Gordon and Breach Science Publishers*, New York, London, Paris, 1956.